

ON DIFFERENT LDPC-BASED JOINT SOURCE-CHANNEL OPTIMISED DECODING SCHEMES

C. Poulliat*, D. Declercq, I. Fijalkow

ETIS - UMR8051
ENSEA/UCP/CNRS
6 avenue du Ponceau
F-95014 Cergy-Pontoise, FRANCE

C. Lamy-Bergot

THALES Land & Joint Systems
EDS/SPM WaveForm Design Group
160 boulevard de Valmy, B.P. 82
F-92704 Colombes Cedex, FRANCE

ABSTRACT

In this paper, we compare different Joint Channel Decoding (JSCD) schemes involving LDPC codes: (i) JSCD optimised, (ii) non-JSCD compatible optimised, and finally (iii) an optimal tandem system assuming perfect source compression. Some Optimisation and simulation results are provided for different rates and codeword lengths.

1. INTRODUCTION

The interest of a joint source-channel receiver is commonly well recognised: it tries to take advantage of both the structure and the residual redundancy of the source. First, [1] consider JSCD for serially concatenated Convolutional Codes and Variable Length Code (VLC) SISO decoders. [2][3] then investigate a doubly iterative system and [4] give an asymptotic convergence analysis of the joint receiver involving an LDPC code that leads to an optimisation method for the LDPC code structure. It is of practical interest to have systems that can perform well both in a JSCD and non-JSCD context for some backward compatibility or less complexity motivations. The question is: how to optimise them and how do they perform? Therefore, in this paper, based on the analysis of [4], we compare different JSCD schemes involving LDPC codes: (i) JSCD optimised, (ii) non-JSCD compatible optimised, and finally (iii) an optimal tandem system assuming perfect source compression. Optimisation and simulation results are provided for different rates and codeword lengths. In Section 2, the overall JSCD system is described. In Section 3, the convergence analysis using the mutual information (MI) evolution technique is briefly reviewed. The optimisation of the JSCD receiver for both JSCD-only and non-JSCD compatible applications is discussed in Section 4. Finally optimisation and simulation results are given in Section 5 and conclusions and perspectives are drawn in Section 6.

*C. Poulliat is granted by the French Lavoisier program. He's currently a post-doctoral fellow at the UHM coding group of the Hawaii university

2. SYSTEM DESCRIPTION AND HYPOTHESIS

In the following, we consider the Binary Input Additive White Gaussian Noise (AWGN) channel as the propagation channel. For practical considerations, we assume that the LDPC code is systematic. A decoding iteration for the global iterative receiver is composed of one LDPC decoding step and one SISO source decoder step and, as in many works, we assume initial synchronisation of the source decoder. The factor graph corresponding to the proposed system is given in Figure 1. Belief propagation (BP) is used

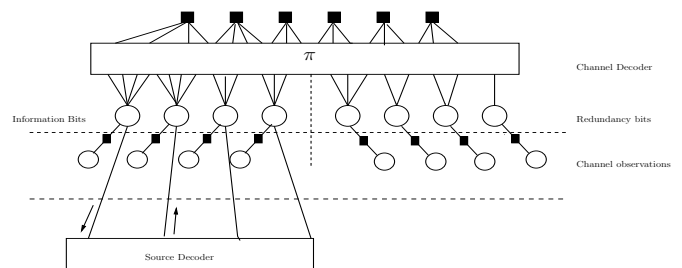


Fig. 1. Graph for the joint LDPC and source decoder.

for the LDPC decoder and Maximum A Posteriori (MAP) decoding through BCJR (equivalent to BP on a VLC factor graph) for the source decoder. For the purpose of the optimisation, infinite length codewords are first considered, but simulation results will be done for both long and medium length codewords, and result analysis carried out in both cases.

3. CONVERGENCE ANALYSIS: A BRIEF REVIEW

In this section, we briefly review the convergence analysis that leads to the optimisation method presented in section 4 (see [4] for more details). We consider the MI associated with the Log-Likelihood ratio (LLR) messages along the edges in the graph (see [5] [6]). As the source decoder pro-

vides an extrinsic information only for information bits, two classes of data nodes are distinguished, namely information and redundancy data nodes. At decoding iteration ℓ , we note respectively $x_{cv}^{(\ell)}$, $x_{vc}^{I(\ell)}(i)$, $x_{vc}^{R(\ell)}(i)$, $x_{vs}^{(\ell)}(i)$ and $x_{sv}^{(\ell)}(i)$ the MI from parity check nodes to variable nodes, the MI from variable nodes with connection degree i to check nodes for information (I) data nodes, the MI from variable nodes with connection degree i to check nodes for redundancy (R) data nodes, the MI from variable nodes with connection degree i to source decoder and the MI from source decoder to variable nodes. We define $x_{vc}^{(\ell)}$ as the MI at the check node input (after the interleaver π). It is thus a mixture of $x_{vc}^{I(\ell)}(i)$ and $x_{vc}^{R(\ell)}(i)$. Using a Gaussian Approximation [7], all MI quantities can be related to the mean of LLR messages with the function $J(\cdot)$ defined as follows [5]

$$J(m) = 1 - \frac{1}{\sqrt{4\pi m}} \int_{\mathbf{R}} \log_2(1 + e^{-v}) \exp\left(\frac{-(v-m)^2}{4m}\right) dv.$$

Considering the LDPC code structure, are denoted by $\underline{\rho} = [\rho_2, \dots, \rho_{t_{r_{\max}}}]^T$, $\underline{\lambda}^I = [\lambda_2^I, \dots, \lambda_{t_{c_{\max}}}^I]^T$ and $\underline{\lambda}^R = [\lambda_2^R, \dots, \lambda_{t_{c_{\max}}}^R]^T$ respectively the proportion of edges connected to check nodes with degree $\{j, j = 2, \dots, t_{r_{\max}}\}$, the proportion of edges connected to information data nodes with degree $\{i, i = 2, \dots, t_{c_{\max}}\}$ and the proportion of edges connected to the redundancy data nodes with connection degree $\{r, r = 2, \dots, t_{c_{\max}}\}$. We also note $\underline{\lambda} = [\underline{\lambda}^I, \underline{\lambda}^R]^T$, $\underline{1}/t_c = [1/2, \dots, 1/t_{c_{\max}}]^T$ and $\underline{1}/t_r = [1/2, \dots, 1/t_{r_{\max}}]^T$. $t_{r_{\max}}$ (resp. $t_{c_{\max}}$) is the highest available connection degree for the check nodes (resp. the data nodes). Considering propagation on an AWGN channel, the mean of channel observations messages is $\mu_0 = 2/\sigma^2$ with σ^2 the noise variance of the channel.

Assuming Gaussian Approximation for both the LDPC decoder and the SISO source decoder, the set of MI evolution equations are:

- variable nodes messages update:

$$\begin{aligned} x_{vc}^{I(\ell)}(i) &= J(\mu_0 + (i-1)J^{-1}(x_{cv}^{(\ell-1)}) + J^{-1}(x_{sv}^{(\ell-1)}(i))) \\ x_{vc}^{R(\ell)}(r) &= J(\mu_0 + (r-1)J^{-1}(x_{cv}^{(\ell-1)})) \\ x_{vc}^{(\ell)} &= \sum_{i=2}^{t_{c_{\max}}} \lambda_i^I x_{vc}^{I(\ell)}(i) + \sum_{r=2}^{t_{c_{\max}}} \lambda_r^R x_{vc}^{R(\ell)}(r) \end{aligned} \quad (1)$$

- check nodes messages update:

$$x_{vs}^{(\ell)} = 1 - \sum_{j=2}^{t_{r_{\max}}} \rho_j J((j-1)J^{-1}(1 - x_{vc}^{(\ell)})) \quad (2)$$

- LDPC decoder to source decoder messages update:

$$x_{sv}^{(\ell)}(i) = J(\mu_0 + iJ^{-1}(x_{vc}^{(\ell)})), \forall i = 2, \dots, t_{c_{\max}} \quad (3)$$

- source decoder messages update:

$$x_{sv}^{(\ell)}(i) = T(x_{vs}^{(\ell)}(i)), \forall i = 2, \dots, t_{c_{\max}} \quad (4)$$

where $T(\cdot)$ is the EXIT chart function of the source decoder, generally estimated using Monte Carlo simulations as done in [8] under a Gaussian Approximation. Equations (1), (2), (3) and (4) give the complete MI evolution

$$x_{vc}^{(\ell+1)} = F([\underline{\lambda}^I, \underline{\lambda}^R], x_{vc}^{(\ell)}, \mu_0) \quad (5)$$

for which the initial conditions are $\forall i = 2 \dots t_{c_{\max}}, x_{sv}^{(0)}(i) = 0$ and $x_{cv}^{(0)} = 0$.

The condition $F([\underline{\lambda}^I, \underline{\lambda}^R], x, \mu_0) > x, \forall x \in [0, 1]$ ensures convergence at the fixed point $x = 1$ for equation (5). If we note $M = J^{-1}(T(1))$, the stability condition at the fixed point, corresponding to zero error probability, can be derived semi-analytically and is given by [4][6]: (i) if $T(1) = 1$: $\lambda_2^R < e^{\frac{1}{2\sigma^2}} / \sum_j \rho_j(j-1)$, (ii) if $T(1) < 1$: $\lambda_2^I e^{-\frac{M}{4}} + \lambda_2^R < \lambda_2^*(\sigma^2, \underline{\rho}) = e^{\frac{1}{2\sigma^2}} / \sum_{j=2}^{t_{r_{\max}}} \rho_j(j-1)$.

It is to be noted that the effect of the desynchronisations in the VLC decoding, and the way the soft source decoder manage it, is in fact taking into account when evaluating the EXIT chart (by averaging the transfer function over all decoded sequences).

4. SYSTEM OPTIMISATION

In this section, different optimisation strategies for a joint source-channel receiver are presented, together with the potential impact on iterative systems, corresponding either to backward compatibility wishes or less complex solutions.

4.1. JSCD-only optimisation

Based on the results of [4], the optimisation of the LDPC code parameters can be written as a linear programming optimisation problem when the maximisation of the code rate R is considered. For $\rho(x)$ and σ^2 fixed, the optimisation can be stated as follows :

$$\underline{\lambda}_{opt} = \max_{\underline{\lambda}} [\underline{1}/t_c, \underline{1}/t_r]^T \underline{\lambda} \text{ with constraints: } (6)$$

$$[C_1] \text{ proportions : } \underline{1}^T \underline{\lambda} = 1 \text{ and } \underline{1}/t_c^T \underline{\lambda}^R = \underline{1}/t_r^T \underline{\rho},$$

$$[C_2] \text{ convergence : } F(\underline{\lambda}, x, \mu_0) > x,$$

$$[C_3] \text{ stability condition : } \lambda_2^I e^{-\frac{M}{4}} + \lambda_2^R < \lambda_2^*(\sigma^2, \underline{\rho}).$$

For a target rate R , by some successive searches on σ^2 and $\rho(x)$, we obtain the best parameters $(\lambda(x), \rho(x))$ that give the best threshold $\delta^* = (E_b/N_0)_{opt}$ under a gaussian approximation.

4.2. Optimisation compatible for non-JSCD systems

For some backward compatibility reasons, one may want to design a channel decoder that can perform well over the AWGN channel both with and without considering iterative interactions with a soft source decoder. When considering LDPC codes, we can find some codes performing close to the AWGN channel capacity using different methods under asymptotic assumptions [7][9]. The association of the information bits with the data nodes having the highest connection degrees would give the best mapping for the AWGN channel, noted \mathcal{M}_0 , in terms of the average Bit Error Rate (BER) for a given iteration number l [7]. This is the one used in [4] to compare optimised and non-optimised JSCD receiver involving an LDPC code.

From a theoretical point of view (*i.e.* asymptotic performance), when considering the threshold as a performance criterion (*i.e.* an infinite number of iterations), any mapping should be equivalent. Therefore, considering another mapping for the AWGN channel does not change the threshold. However, this is not true for the JSCD receiver since: (i) there is clearly a dissymmetry in the message passing between the variable nodes associated with information and redundancy bits, (ii) considering the stability condition C_3 , one understands that there may exist a code that satisfies the convergence condition C_1 and having a repartition of the 2-connected variable nodes between information and redundancy bits that gives a better threshold than with the mapping \mathcal{M}_0 (*i.e.* all low-connected nodes are associated with the redundancy). Thus, the question is: what is the best mapping to use when considering the AWGN optimised code as a component of the joint receiver? By considering the optimisation method (6), the optimal mapping in terms of threshold can be obtained by just adding a constraint on the code profile. This is given by: $[C_4] \forall k = 2 \dots t_{c_{\max}}, \lambda_k^I + \lambda_k^R = \lambda_k^{(a)}$. $\lambda_k^{(a)}$ is the proportion of edges connected to a variable node with degree k for the AWGN optimised code. Let \mathcal{M}^* be the mapping obtained.

5. RESULTS

In this section, some optimisation results are presented. Without loss of generality, we consider a SISO Variable Length Code (SISO-VLC) as the source decoder. The VLC code considered as our example and the corresponding independent symbols source are taken from [1]: it consists of the codebook $\mathcal{C} = (00, 11, 010, 101, 0110)$ with associated probabilities $\mathcal{P} = (0.33, 0.30, 0.18, 0.10, 0.09)$. The associated entropy and VLC average length are respectively $H = 2.14$ and $\bar{l} = 2.46$ bits/symbols. The residual source redundancy is given by $R_s = H/\bar{l} = 0.86992$. The SISO-VLC source decoder is a Bit-level MAP VLC soft decoder introduced by [10]. The extrinsic MI transfer function is esti-

mated through Monte Carlo simulations as in [8]. For the VLC code used, simulated EXIT charts gives the condition $T(1) \simeq 1$. We consider concentrated degrees distribution for $\rho(x)$ [7]. We perform the optimisation for different values of $\bar{\rho} = \rho j + (1 - \rho)(j + 1)$ to obtain the code with the best decoding threshold for $t_{c_{\max}} = 30$, $R = 1/2$ and $R = 2/3$. The overall redundancy rate is given by $R_T = R_s R = 0.43496$ for the code with the coding rate $R = 1/2$ and $R_T = 0.5799$ for the code with the coding rate $R = 2/3$. At rate R_T , the Shannon limit for AWGN channel gives the theoretical information bit energy to noise ratio $E_b/N_0 = -0.0957$ dB and $E_b/N_0 = 0.5734$ dB for $R_T = 0.43496$ and $R_T = 0.5799$ respectively.

5.1. JSCD-only optimisation results

The Figure 2 gives the theoretical threshold of the **joint receiver** $\delta^* = 1/(2 * R_T * \sigma^2)$ as a function of $\bar{\rho}$ for $R = 1/2$ and $R = 2/3$. For both, there exists a minimum value δ^* that gives the best code parameters $(\lambda(x), \rho(x))$ for the JSCD system. The dashed horizontal lines are the theoretical information bit energies to noise ratio given by Shannon limit. For $R = 1/2$ and $R = 2/3$, the optimal values that minimise the threshold are $\bar{\rho} = 7.91$ $\bar{\rho} = 12.46$. The obtained data node connection profiles are given in Table 1.

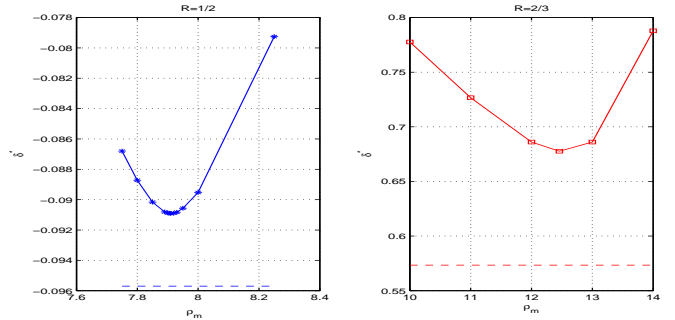


Fig. 2. δ^* as a function of $\rho_m = \bar{\rho}$

5.2. Non-JSCD optimisation results

First, we optimise the profile for the AWGN channel for $t_{c_{\max}} = 30$, $R = 1/2$ and $R = 2/3$ using a Gaussian approximation [7] using mutual information evolution [6]. For each rate, we deduce the mappings \mathcal{M}_0 and then \mathcal{M}^* , applying the optimisation method (6) with the additional constraint C_4 . The obtained results are given in the Table 2. Whereas we find a mapping different from \mathcal{M}_0 that minimises the threshold for $R = 1/2$, we find for $R = 2/3$ that the mapping \mathcal{M}_0 gives finally the best threshold. From these results, it can be concluded that mappings giving better threshold than \mathcal{M}_0 can be found. Still, it is to be noted

$\lambda(x)$	$R = 1/2$		$R = 2/3$	
	I	R	I	R
λ_2	0.1130	0.2216	0.1896	0.1608
λ_3	/	0.0475	/	/
λ_4	0.0830	/	/	/
λ_5	0.1201	/	0.1837	/
λ_7	/	/	0.0635	/
λ_9	0.0588	/	0.0306	/
λ_{10}	0.1044	/	0.0145	/
λ_{10}	/	/	0.0587	/
λ_{30}	0.2516	/	0.2986	/

Table 1. Left degree distributions for JSCD optimised codes.

that the difference will probably be only located in the low-st degrees, as it is shown for $R = 1/2$ in Table 2.

$\lambda(x)$	$R = 1/2$		$R = 2/3$		$R = 2/3$	
	\mathcal{M}^*		\mathcal{M}_0		$\mathcal{M}_0 = \mathcal{M}^*$	
	I	R	I	R	I	R
λ_2	0.0080	0.2022	/	0.2102	0.0348	0.1345
λ_3	0.1641	0.0301	0.1777	0.0165	0.2011	/
λ_5	0.0435	/	0.0435	/	0.0008	/
λ_7	0.1400	/	0.1400	/	0.1964	/
λ_8	0.1044	/	0.1044	/	0.0926	/
λ_{30}	0.3036	/	0.3036	/	0.3388	/

Table 2. Non-JSCD compatible schemes: Left degree distributions and repartition.

5.3. Simulation results

For the practical decoding, we use the following rule: the iterative decoding is performed until we find a valid codeword through syndrome computation after each iteration or the number of iterations exceed a maximum number of global iterations. In our simulations, the maximum number of iterations is set to 150. We now examine simulation results for long and medium size codewords. In both cases, the length of codeword is chosen carefully in order to have the same number of source symbols per frame. This allows us to compare Frame Error Rate (FER) as well as BER for the different rates and receiver systems we consider. We compare four schemes for the two different rates :

- (i) Optimal joint source channel receiver (JSCD-opt).
- (ii) Joint source-channel receiver using AWGN optimised code using the information mapping \mathcal{M}_0 (JSCD- \mathcal{M}_0).
- (iii) Joint source-channel receiver using AWGN optimised code using the information mapping \mathcal{M}^* (JSCD- \mathcal{M}^*) (only for $R_T = 0.43496$ according to section 5).

(iv) Tandem scheme (TS-opt): we consider a perfectly compressed source coded by the AWGN optimised LDPC code with code rate R_T . This intends to correspond to the scheme induced by the Shannon's separation theorem under asymptotic assumptions.

NB: BER for the scheme TS-opt is difficult to compare to the other schemes since it does not represent the same quantity of information but it is still given.

5.3.1. Long size codewords

In figure 3, when studying both BER and FER curves, we can see that as expected JSCD schemes performs better than JSCD- \mathcal{M}^* and JSCD- \mathcal{M}_0 . In both cases, there is an improvement of about 0.4 dB. JSCD- \mathcal{M}^* and JSCD- \mathcal{M}_0 finally perform closely from each other. It can be observed that the difference between JSCD-opt and TS-opt is less for $R_T = 0.43496$ than for $R_T = 0.5799$. JSCD-opt scheme performs for FER performance at less than 0.1 dB from the TS-opt scheme for $R_T = 0.43496$, and at 0.15 dB for $R_T = 0.5799$: the JSCD goal seems to be achieved for this source, *i.e* an efficient exploitation of the residual redundancy to perform as close as possible to the limit given by the TS-opt scheme. It should be remarked that the role of JSCD optimisation is to take into account the unavoidable presence of residual redundancy factor in a real source. As such, the problem is not the actual source redundancy factor, but the capacity to build a joint receiver that can exploit efficiently this residual redundancy.

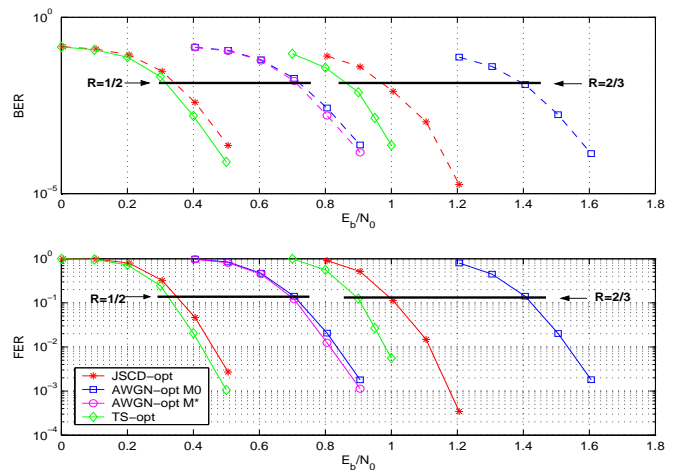


Fig. 3. BER and FER for long codeword: $N = 30000$ and $N = 22500$ for $R = 1/2$ and $R = 2/3$ resp.

5.3.2. Medium size codewords

Considering now medium length codewords, the results presented in Figure 4 show that FER performance improves

when comparing JSCD- \mathcal{M}^* and JSCD- \mathcal{M}_0 with JSCD-opt which performs itself very closely to TS-opt. As for Figure 3 curves, it is observed that the difference between JSCD-opt and TS-opt is greater for $R_T = 0.5799$ than $R_T = 0.43496$. However, contrarily to the behavior observed for long codewords, the simulations carried for medium length codewords make appear an error floor around 10^3 for FER curves, and a reduction of the curve slope for BER curves. The presence of error floor is frequently observed for medium finite size codewords in iterative systems, but does not induces the asymmetry between BER and FER curves which can be explained by the fact that the SISO source decoder is a bit-level trellis MAP decoder, which minimises the BER but does not guarantee minimised FER. The TS-opt is not subject to this asymmetry, eventhough the effect of finite size induces low convergence. Further studies will try to give a better understanding of the error floor region, and solutions to help lowering error floor.

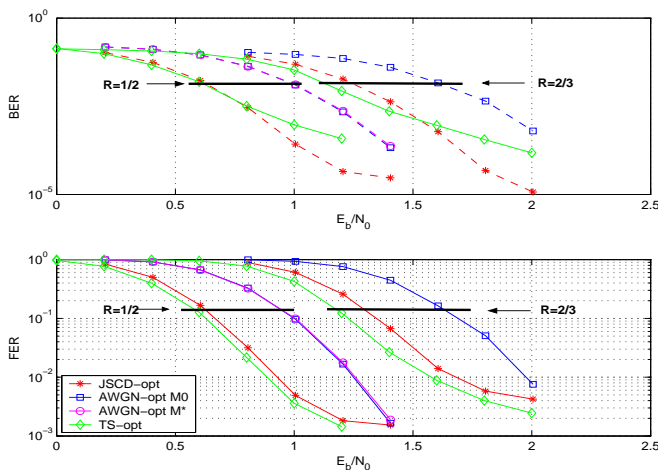


Fig. 4. BER and FER for medium codeword size: $N = 4096$ and $N = 3072$ for $R = 1/2$ and $R = 2/3$ resp.

6. CONCLUSION

In this paper, different joint source-channel decoding schemes involving an LDPC decoder as a channel code component are compared for different rates and codeword sizes. Simulations results show that JSCD-optimised scheme perform well for long codeword size, but can exhibit frame error floor for medium size. When considering a non-JSCD compatible receiver, an optimal mapping can be determined, but simulation results show that the improvement is only little when compared to the natural mapping used for AWGN channel. This seems due to the fact that the mapping only differs by their lowest degrees. Further studies will investigate the error floor region, to have a better understanding of the joint decoder behavior in order to have some guidelines

to optimise code for small codeword size. The study can be extended to sources with a different residual redundancy, in order to see its influence: this would allow to define rules to manage the tradeoff between the redundancy to allocate to the source and the channel code.

7. REFERENCES

- [1] R. Bauer and J. Hagenauer, "On variable length codes for iterative source/channel decoding," in *IEEE Data Comp. Conf. (DCC)*, Snowbird, UT, USA, Mar. 2001, pp. 272–282.
- [2] L. Guivarch, J.C. Carlach, and P. Siohan, "Joint source-channel soft decoding of Huffman sources with turbo-codes," in *IEEE Data Comp. Conf. (DCC)*, Snowbird, UT, USA, Mar. 2000, pp. 83–92.
- [3] X. Jaspard and L. Vandendorpe, "New iterative decoding of variable length codes with turbo codes," in *IEEE Int. Conf. on Com.*, Paris, France, Jun. 2004.
- [4] C. Poulliat, D. Declercq, C. Lamy-Bergot, and I. Fijalkow, "Analysis and optimization of irregular LDPC codes for joint source-channel decoding," *IEEE Com. Letters*, Accepted for publication, November 2004.
- [5] S. ten brink, "Convergence behavior of iteratively decoded parallel concatenated codes," *IEEE Trans. on Com.*, vol. 49, no. 10, pp. 1727–1737, Oct. 2001.
- [6] A. Roumy, S. Guemghar, G. Caire, and S. Verdú, "Design methods for irregular repeat-accumulate codes," *IEEE Trans. on Inf. Theory*, vol. 50, no. 8, pp. 1711–1727, Aug. 2004.
- [7] S.Y. Chung and T.J. Richardson R.L. Urbanke, "Analysis of sum-product decoding of low-density parity-check codes using a gaussian approximation," *IEEE Trans. on Inf. Theory*, vol. 47, no. 2, pp. 657–670, Feb. 2001.
- [8] J. Hagenauer and R. Bauer, "The turbo principle in joint source channel decoding of variable length codes," in *IEEE Inf. Theory Work.*, Cairns, Australia, Sept. 2001, pp. 128–130.
- [9] T.J. Richardson, M.A. Shokrollahi, and R.L. Urbanke, "Design of capacity-approaching irregular low-density parity-check codes," *IEEE Trans. on Inf. Theory*, vol. 47, no. 2, pp. 619–637, Feb. 2001.
- [10] V.B. Balakirsky, "Joint source and channel decoding with variable length codes," *Prob. of Inf. Trans.*, vol. 27, no. 1, pp. 12–27, 2001.